Experiments with Tunnel Junctions Using Ferromagnetic Metals

J. E. CHRISTOPHER, R. V. COLEMAN, ACAR ISIN, AND R. C. MORRIS
Department of Physics, University of Virginia, Charlottesville, Virginia
(Received 13 March 1967; revised manuscript received 27 December 1967)

Results on tunnel current flow in junctions using ferromagnetic metals as electrodes or as added impurities at the barrier electrode interface are reported in this paper. Oxides of the ferromagnetic metal and aluminum oxide have been used to form the insulating barrier in combination with a second electrode made from aluminum, silver, or iron. Complete data are reported for various types of junctions using iron and iron oxide and covering a zero-bias resistance range at 4.2°K from 10^{-1} Ω to above 10^{8} Ω. Preliminary results on junctions using cobalt and nickel are also reported. The most general feature of interest is a very strong non-Ohmic behavior at low bias voltage and a very rapid temperature dependence of tunnel conductance, particularly in the helium temperature range. Data obtained on Al–Al_2O_3–Al junctions doped with iron impurities at the Al_2O_3–Al interface show a strong zero-bias anomaly corresponding to a resistance maximum. This behavior appears to be generally explained by an anomalous scattering mechanism near zero bias and has been compared to the behavior of identical undoped Al–Al_2O_3–Al junctions. The experiments on junctions using iron oxide barriers also show strong zero-bias anomalies, but in addition show a more complex temperature dependence and an unusual breakdown effect at high voltages. These latter features are possibly associated with special properties of magnetic iron oxide Fe_3O_4. The data on junctions with iron oxide barriers have also been compared to the behavior predicted by standard tunnel theory, and areas of qualitative agreement can be found if a relatively low barrier height is assumed. The appropriate barrier height has been estimated as 0.025 eV from Fowler-Nordheim plots of the data. The preliminary data on junctions made with CoO_x and NiO_x barriers also show some similar effects, but they are generally of smaller magnitude. The experimental data will be presented in detail along with a summary of the relevant theories.

INTRODUCTION

MEASUREMENTS have been made of the current flow through normal metal tunnel junctions in which a ferromagnetic metal has been used on either one or both sides of the junction. In addition, measurements have been made on Al–Al_2O_3–Al junctions in which a small amount of iron has been evaporated onto the oxide-metal interface. In the case of junctions made with iron electrodes the insulating layer has been either iron oxide or aluminum oxide and various combinations of metal electrodes have been used, including electrodes made from Al, Fe, Ag, and Au. Data on Co–CoO_x–Al and Ni–NiO_x–Al are also reported, although the most complete data have been obtained on junctions using iron films.

The junctions used in these experiments have shown such extreme voltage and temperature dependence that the behavior can be characterized as anomalous, in similarity to zero-bias anomalies previously observed in junctions such as Cr–CrO_x–Ag.[1]

In general, the junctions show zero-bias anomalies at helium temperatures corresponding to strong resistance maxima. The resistance maxima also show a strong temperature dependence, which can be observed even at temperatures down to 1°K.

For the junctions made with pure FeO_x barriers, a number of features associated with the special properties of iron oxide have also been observed. These include tunneling through thick layers of iron oxide (of the order of 1000 Å) and an unusual "breakback" effect. The resistance also shows an extremely rapid decrease between 4.2 and 77°K, possibly associated with a transition in magnetic iron oxide.

We have made a general comparison of all the data to the predictions of anomalous tunneling theory[2] and find a general qualitative agreement. In the case of FeO_x barriers, we have also analyzed the data to determine possible areas of agreement with standard tunneling theory.[3] We find that some of the data on iron oxide barriers are not inconsistent with a standard tunneling process and an unusually low barrier height, although this alternative is at present speculative. In this paper we discuss the various experiments in detail along with a general comparison to theoretical predictions. A summary of the theoretical work is also included.

For convenience we will divide the experiments into two general classes depending on the resistance range of the junction. These ranges will correspond to zero-bias resistances measured at 4.2°K of less than 10^3 Ω for the low-resistance junctions and greater than 10^3 Ω for the high-resistance junctions. The characteristic curves for these two ranges of resistance often show a different appearance, but this may simply be due to the large difference in the variable range used or to possible differences in the oxide structure. The resistance ranges are obtained by simply varying the time and temperature of oxidation during preparation. In the case of Ni and Co, only junctions in the low-resistance range have been studied.

Characteristic voltage versus current and dV/dI (dynamic resistance) versus voltage curves have been

[1] J. M. Rowell and L. Y. L. Shen, Phys. Rev. Letters **17**, 15 (1966).

[2] J. Appelbaum, J. C. Phillips, and G. Tzouras, Phys. Rev. **160**, 554 (1967).

[3] J. G. Simmons, J. Appl. Phys. **34**, 2581 (1963).

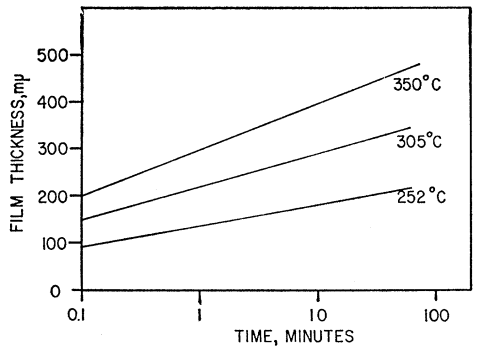

FIG. 1. Iron oxide film thickness as a function of time for oxidation of iron in air at 252, 305, and 350°C (see Ref. 4).

recorded for a range of temperature from 1°K to room temperature.

In most cases we observe a resistance maximum at zero bias and increase of either temperature or voltage decreases the resistance rapidly. The magnitude of this drop over the range of voltage used is of the order of 10 for the low-resistance junctions and of the order of 10^6 for the high-resistance junctions.

We will outline the experimental techniques and results in the following sections and then discuss the comparison with theory. The complete data on various types of junctions involving iron will be presented first, and a separate section will include the results on nickel and cobalt. The comparison to theory will apply mostly to iron since the results on nickel and cobalt are still of a preliminary nature.

EXPERIMENTAL TECHNIQUES

The samples were made by vacuum deposition onto glass substrates. Both a standard high-vacuum oil system and a Varian vac-ion system were used for the evaporation. In all cases the ferromagnetic films were evaporated using a hot filament of the metal made from a 0.020-in. wire with a purity of 99.99+%. In the case of the nonmagnetic electrodes the evaporation was performed by heating the metal in a tungsten heater using metal of 99.999% purity. During the evaporation the pressure was approximately 10^{-6} Torr in the oil system and 10^{-7} Torr in the Varian system. In most cases no appreciable difference was observed for similar junctions prepared in the different vacuum systems.

The junctions were prepared in the form of an X and the overlap area of the two electrodes was of the order of 1.5 to 2 mm^2. The insulating oxide layer was formed by oxidizing the base electrode in air at atmospheric pressure for a range of temperature from 27 to 350°C. Oxidation times from 5 min to 300 h have been used. The low-resistance junctions were formed by oxidation in the lower range of temperatures, while the high-resistance junctions were generally formed at oxidation temperatures above 200°C.

The oxide layer thickness has not been measured directly, but for purposes of analysis we have used published curves for oxide thickness as a function of time and temperature. In the case of iron we have used data published by Tomashov[4] and reproduced in Fig. 1. These curves have been used to estimate the thickness of the oxide layers for a number of the junctions discussed in this paper and these estimates can be found in Table I. Other published data[5] show reasonable agreement with the results shown in Fig. 1, although a survey of the literature shows a fairly wide variation in the results reported by different investigators.

The voltage-current curves were recorded on a Moseley X-Y recorder and in the case of the high-resistance junctions a unity gain, high input impedance amplifier was used between the voltage leads and the X-Y recorder.

The dynamic resistance versus voltage was measured using a PAR HR-8 lock-in amplifier. The ac voltage observed for a fixed ac current was measured and this voltage was calibrated in terms of resistance by using a known standard resistor.

Standard low-temperature cryostats were used for the measurements in the helium temperature range. The junctions were immersed in the helium bath and temperatures were measured using helium vapor-pressure values.

EXPERIMENTAL RESULTS ON LOW-RESISTANCE IRON JUNCTIONS

Junctions with resistances less than 10^3 Ω were obtained by oxidizing the iron films at relatively low temperatures and for short times. Preliminary results on junctions with resistance values of 0.1–150 Ω have been reported by Isin *et al.*[6] and in the case of Fe–FeO_x–Al junctions a giant zero-bias anomaly corresponding to a resistance maximum was observed as shown in Fig. 2. The data were obtained at 1.1°K and the curves correspond to data taken with the aluminum electrode in the superconducting state at $H=0$ and in the normal state with a sufficiently high magnetic field to quench the superconductivity. The dotted section of the curve shows the extra zero-bias resistance obtained when the aluminum is superconducting and clearly shows the existence of the energy gap in the aluminum. This also indicates that some or possibly all of the current is flowing via a tunneling mechanism.

Magnetic fields on the order of 1–10 kOe were sufficient to quench the superconductivity in the aluminum, and the smooth solid curve of Fig. 2 was obtained with the aluminum in the normal state. In order to check the superconducting transition in the aluminum film we have also made measurements of the dc resist-

[4] N. D. Tomashov, *Theory of Corrosion and Protection of Metals* (The MacMillan Co., New York, 1966), p. 55.
[5] U. R. Evans, *An Introduction to Metallic Corrosion* (Edward Arnold and Co., London, 1950), p. 10.
[6] A. Isin, J. E. Christopher, and R. V. Coleman, J. Appl. Phys. **39**, 704 (1968).

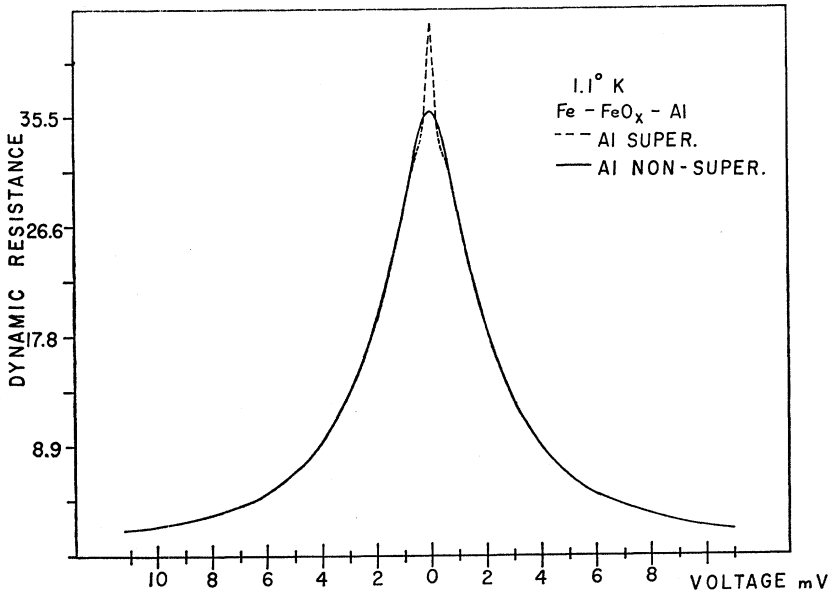

FIG. 2. Dynamic resistance as a function of voltage at 1.1°K for an Fe–FeO$_x$–Al junction. The superconductivity of the aluminum was quenched with an external magnetic field to obtain the solid curve. Dashed curve shows data obtained with aluminum in the superconducting state.

ance simultaneously with the tunnel-current measurement and find satisfactory correlation. Transition temperatures up to 2°K have been observed and in general the transition from normal resistance to zero resistance is spread out over a range ΔT of 0.1 to 0.5°K. For all aluminum films used so far, fields greater than 10 kOe completely quench superconductivity.

For applied magnetic fields above the critical quenching field very little change in the characteristic curve was observed as shown for 2.7°K in Fig. 3. Figure 3 also shows a series of dynamic-resistance-versus-voltage curves obtained at progressively lower temperatures in an applied field of 50 kOe. Over a range of 0.6°K a very rapid increase of the zero-bias resistance was observed.

The shape of the temperature-dependence curve for zero-bias resistance in a given temperature range is a function of specific junction preparation, but over the range from 1 to 300°K the low-resistance junctions all show the same general temperature dependence and typical data are shown in Fig. 4. The solid curves in the figure show either zero-bias resistance or conductance as a function of the logarithm of the temperature. The X's in the figure are resistance values at 1.6°K computed from the formula $X=R(T)=R(1.6°K+2850\ V)$. This analysis gives a temperature equivalent of the voltage dependence of resistance and indicates that voltage and temperature are to some extent equivalent variables in regard to their effect on the dynamic resistance.

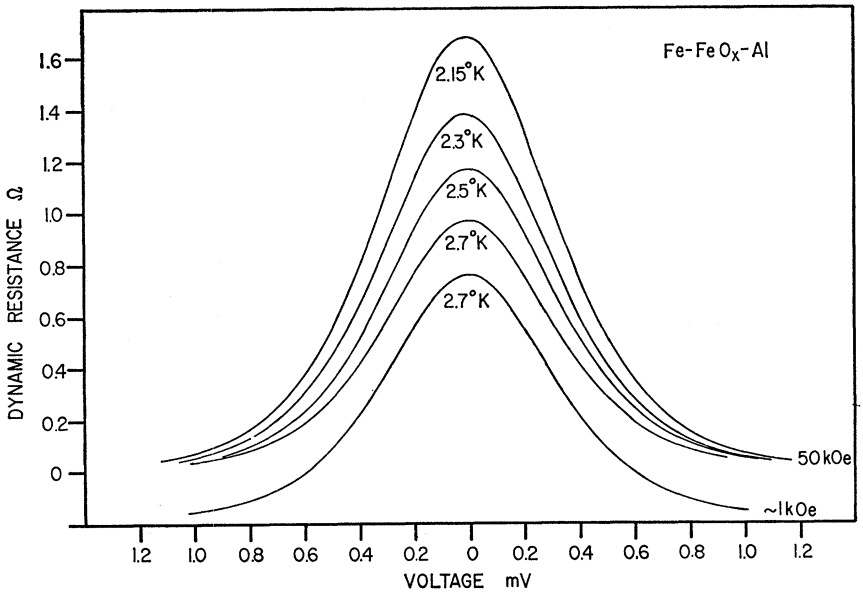

FIG. 3. Dynamic resistance as a function of voltage for an Fe–FeO$_x$–Al junction. The resistance is shown for the temperature range 2.15 to 2.7°K for an external magnetic field of 50 kOe. The zero of resistance for the data at 2.7°K and 1 kOe is shifted downward one division.

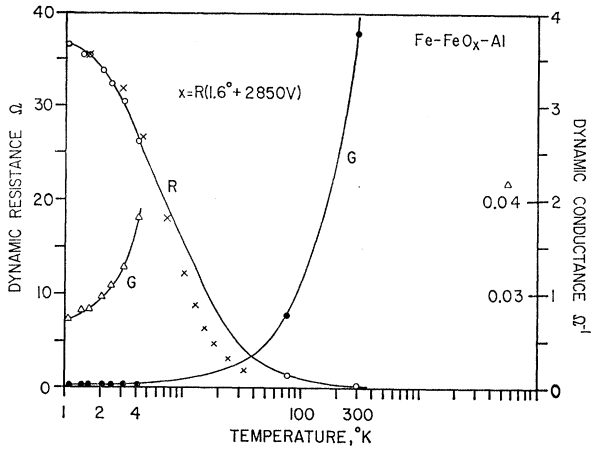

FIG. 4. Temperature dependence of the zero-bias resistance and conductance over the temperature range 1 to 300°K. Also plotted is the voltage dependence of the dynamic resistance at 1.6°K using a fitted temperature equivalence of voltage (×'s).

The conductance as a function of voltage in the helium temperature range can be varied over a fairly wide range depending on the specific junction preparation. Data for a typical Fe–FeO_x–Al junction are shown in Fig. 5. Data obtained on a Cr–CrO_x–Ag junction by Rowell and Shen[1] are also shown for comparison.

In the case of the FeO_x junctions when the second metal electrode is not made from aluminum, but from silver or iron, the corresponding junction resistance is much lower for oxidizing conditions equivalent to those used for junctions with the second electrode made from aluminum. This observation led us to make junctions with much thicker layers of iron oxide and we have obtained results on these with the second metal electrode made from Fe, Al, and Ag. These junctions generally have zero-bias resistances at 4.2°K orders of magnitude larger than those just discussed and their behavior will be summarized in the next section.

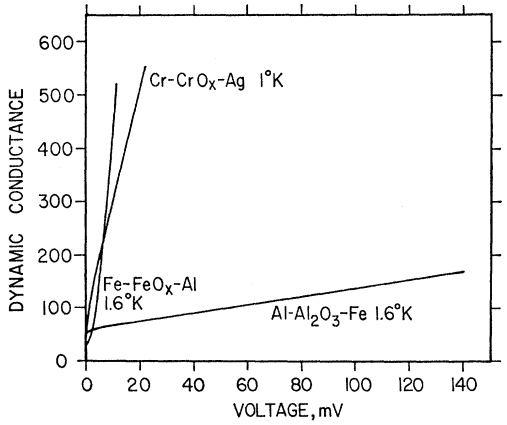

FIG. 5. Dynamic conductance in arbitrary units in the helium temperature range as a function of voltage for several junctions. (Cr–CrO_x–Ag) data obtained from Rowell and Shen (see Ref. 1).

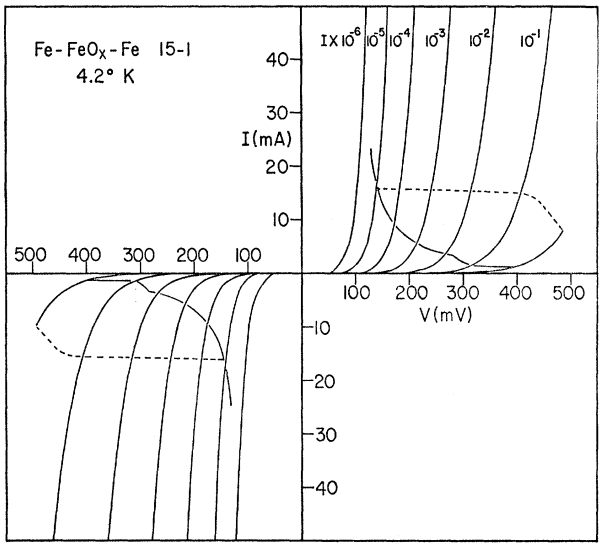

FIG. 6. Voltage-current characteristic curve for an Fe–FeO_x–Fe junction at 4.2°K.

EXPERIMENTAL RESULTS ON HIGH-RESISTANCE IRON JUNCTIONS

In this case we generally mean junctions with a zero-bias resistance at 4.2°K greater than 10^3 Ω. The higher resistance is obtained by oxidizing for longer times and generally at temperatures considerably above room temperature. Many of these films show yellow to blue interference colors after oxidation.

Typical current-versus-voltage curves recorded at 4.2°K are shown for a Fe–FeO_x–Fe junction in Fig. 6 and for a Fe–FeO_x–Ag junction in Fig. 7. The current increases smoothly and rapidly for applied voltages up

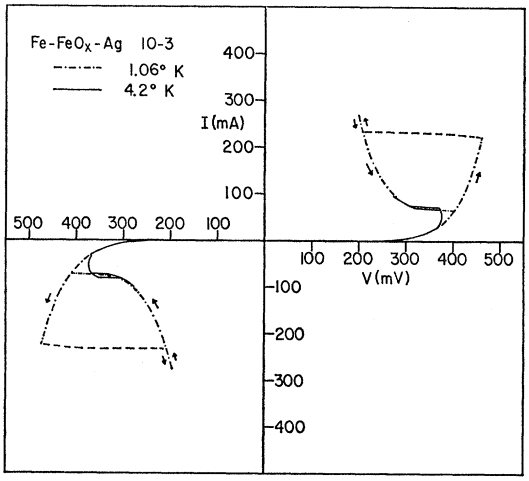

FIG. 7. Voltage-current characteristic curve at high currents for an Fe–FeO_x–Ag junction at 4.2 and 1.06°K. The behavior of this junction was similar to that shown in Fig. 7, but the low currents scales were omitted for clarity. Hysteresis in the "break-back" phenomena is also clearly shown.

to some critical value. Above this critical applied voltage we observe sharp breaks in the current-versus-voltage curve corresponding to a sudden drop in the voltage required to maintain a given current. This phenomena is probably associated with some type of breakdown and is similar to a phenomena sometimes called "breakback" exhibited in the current-versus-voltage curves of commercially available semiconductor devices.[7]

For a given junction the "breakback" behavior is perfectly reproducible over many cycles provided the current is not increased to such a level that damage to the junction results. As shown in Figs. 6 and 7, the behavior above the breakdown point shows a definite hysteresis and the area of the hysteresis loop increases as the temperature is lowered below 4.2°K. (See Fig. 7.)

The extremely large zero-bias resistance observed in these junctions falls rapidly for temperatures above helium temperature and generally is less than a few ohms at 77°K.

The characteristic curves observed at 4.2°K for the Fe–FeO_x–Fe junctions are always symmetrical with respect to a change in polarity of the voltage. This was also true to a high degree for junctions where Al or Ag was used as the second electrode.

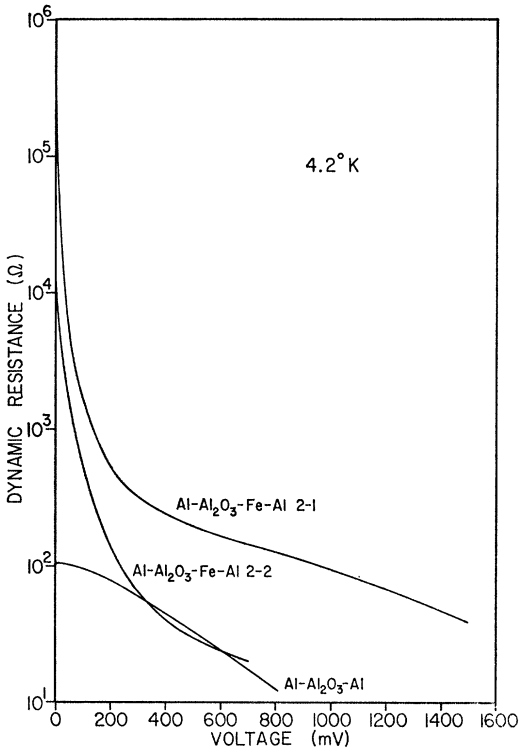

FIG. 8. Dynamic resistance at 4.2°K as a function of voltage for an Al–Al_2O_3–Al and two Al–Al_2O_3–Fe–Al junctions. The three junctions were prepared under identical conditions except for the amount of iron deposited on the the Al_2O_3–Al interface. The amount of iron in sample Al–Al_2O_3–Fe–Al 2-1 is estimated to be enough to be several monolayers and in sample Al–Al_2O_3–Fe–Al 2-2 to amount to less than a monolayer.

[7] Ovonic threshold switches manufactured by Energy Conversior Devices Inc., Troy, Mich.

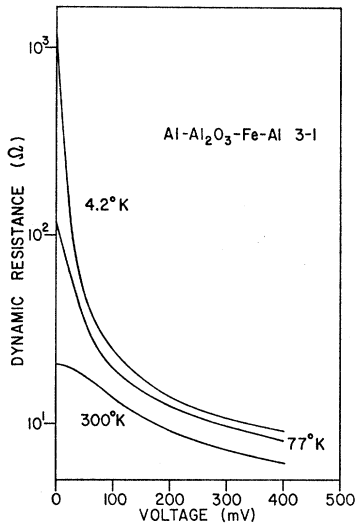

FIG. 9. Dynamic resistance as a function of voltage at 4.2, 77, and 300°K for an Al–Al_2O_3–Fe–Al junction. The amount of iron is estimated to be enough to be several monolayers.

EXPERIMENTAL RESULTS ON JUNCTIONS WITH Al_2O_3 BARRIERS

Tunnel junctions with aluminum oxide barriers also show anomalous behavior when iron is used either as a second electrode or is evaporated onto the barrier in small amounts before the second electrode is evaporated. For the aluminum oxide barriers, the barrier height is estimated to be on the order of 2 eV so that any zero-bias anomaly would most probably be connected with an anomalous tunneling mechanism. Data for Al–Al_2O_3–Al tunnel junctions doped with small quantities of iron are shown in Fig. 8. This plot shows the dynamic resistance as a function of applied bias voltage measured at 4.2°K. Results for a pure Al–Al_2O_3–Al junction prepared at the same time and under identical conditions are also shown for comparison. The data clearly show that the iron impurity adds a strong zero-bias anomaly corresponding to a resistance maximum. The iron-doped junction labeled No. 2-2 is estimated to have less than a monolayer of iron deposited at the junction interface. At high voltages the characteristic curve approaches that of the pure Al–Al_2O_3–Al junction. The iron-doped junction labeled No. 2-1 has considerably more iron added and shows a much higher resistance over the whole range of applied voltage including a sharply rising zero-bias anomaly. The zero-bias anomalies observed in the doped junctions persist up to room temperature and Fig. 9 shows data at 4.2, 77, and 300°K. The voltage and temperature dependence of resistance for these junctions is similar to that observed

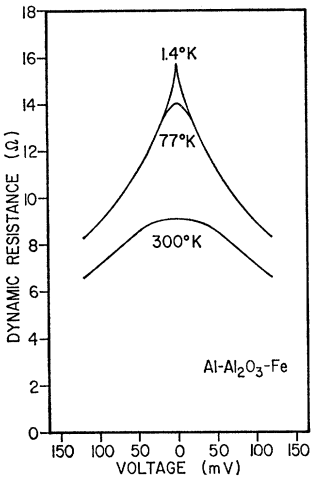

FIG. 10. Dynamic resistance as a function of voltage for an Al–Al_2O_3–Fe junction at 1.4, 77, and 300°K.

for other doped junctions, for example, Al–Al_2O_3–Ag doped with Cu and Ti ions.[8]

Similar but less pronounced effects are observed when iron is used as the second electrode with an undoped Al_2O_3 barrier. Typical data on the dynamic resistance as a function of bias voltage are shown in Fig. 10 for an Al–Al_2O_3–Fe junction at 4.2, 77, and 300°K. The voltage dependence of conductance for this junction is also included in Fig. 5.

EXPERIMENTAL RESULTS ON JUNCTIONS WITH COBALT AND NICKEL FILMS

In view of the fairly striking results obtained with iron electrodes and iron oxide barriers we also made preliminary studies on junctions using cobalt and nickel films. In both cases we were able to obtain resistance maxima at zero bias, although the amplitude as well as the voltage and temperature dependence were much less dramatic than was the case for junctions using iron films. Results were obtained for junctions in which the insulating barrier was an oxide of the ferromagnetic metal formed on the base electrode and aluminum was used as the second electrode. Zero-bias resistances at 4.2°K ranged up to about 150 Ω for the junctions studied so far. In the case of nickel we were also able to obtain a resistance minimum at zero bias when rather impure starting material was used, ~99.9% pure.

Dynamic-resistance-versus-voltage curves for cobalt and nickel are shown in Fig. 11. The temperature dependence of the zero-bias resistance from 1 to 300°K is shown in Fig. 12 for the same three junctions as shown in Fig. 11. In the helium temperature range the temperature dependence is rather weak with a fairly rapid temperature dependence above 77°K. The impure nickel junction with the resistance minimum at zero

[8] A. F. G. Wyatt and D. J. Lythall, Phys. Letters **25A**, 541 (1967).

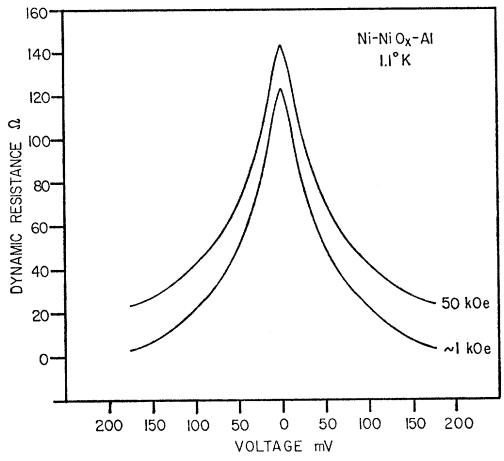

(a)

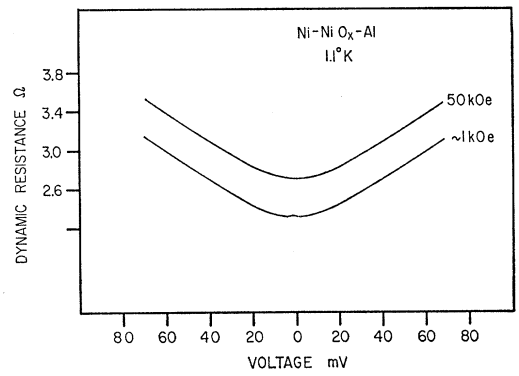

(b)

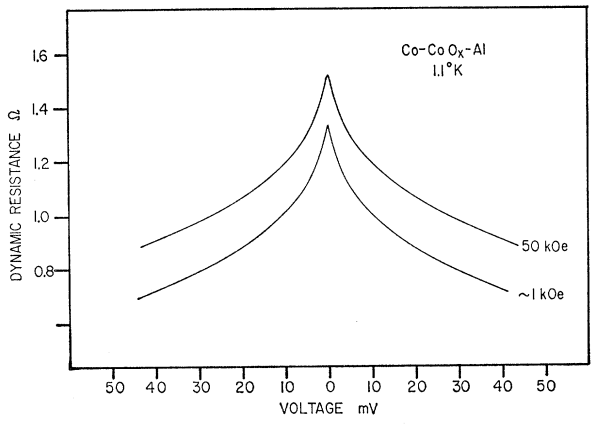

(c)

FIG. 11. Dynamic resistance versus voltage for Ni–NiO_x–Al and Co–CoO_x–Al junctions at 1.1°K in magnetic fields of 1 and 50 kOe. The resistance values refer to the 50-kOe curves and curves for 1 kOe are displaced one division downward.

bias also shows a reverse temperature dependence as indicated in the lower curve of Fig. 12.

Although these data indicate a behavior having some similarities to that obtained with iron film junctions, we would like to emphasize that the results are only preliminary and are not so well established as the results being reported for iron. The oxides of Co and Ni are generally reported to be good insulators in contrast to the magnetic phase of iron oxide (Fe_3O_4), which shows a substantial conductivity at room temperature. This fact, among others, would possibly account for differences in behavior, but definite conclusions will require further study.

THEORY OF TUNNEL EFFECT

The theory of the tunnel effect has been developed by many authors over the past 30 years beginning with the work of Sommerfeld and Bethe[9] and including work by Holm.[10] In recent years considerable work has been applied to the problem where one or both metal electrodes are in the superconducting phase. This problem has been considered by Bardeen[11] and also by Shapiro *et al.*,[12] who have worked out fairly detailed expressions for the tunnel current flow within the framework of the BCS theory. The standard tunnel problem has also recently been examined in detail by Simmons,[3,13] who has developed expressions for the tunnel current flow between normal metal electrodes made from both similar and dissimilar metals. Modifications to Simmons's results have been made by Hartman,[14] who considers detailed quantitative expressions and comparisons to other theories. These are in qualitative agreement with Simmons's original results,

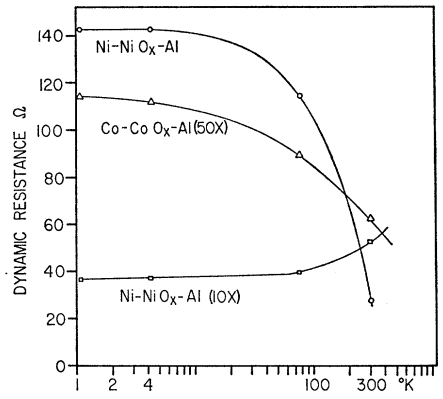

FIG. 12. Temperature dependence of the zero-bias resistance for Ni–NiO_x–Al and Co–CoO_x–Al junctions.

but are more exact if detailed quantitative comparisons are desired. Our results have so far been compared qualitatively to Simmons's original expressions.

In addition to the work mentioned above, Appelbaum,[15,16] Anderson,[17] and Appelbaum *et al.*[2] have developed theories to explain zero-bias anomalies observed in normal metal tunnel junctions. These theories have been suggested as possible explanations for the zero-bias anomalies observed in Ta–TaO_x–Al junctions by Wyatt[18] and by Rowell and Shen.[19] The most recent strong-coupling theory[2] also has possible application to the giant anomalies observed in Cr–CrO_x–Ag by Rowell and Shen,[1] in Al–Al_2O_3–Ag doped with Cu and Ti ions observed by Wyatt and Lythall,[8] and in Al–Al_2O_3–Al doped with Cr impurities observed by Mezei.[20] Sólyon and Zawadowski[21] have also developed a theory giving similar results to those derived by Appelbaum *et al.*,[2] but using an entirely different approach.

In this section we will review briefly the main results of the theories developed by Appelbaum[15,16] and Appelbaum *et al.*[2] and then discuss the standard normal metal tunneling problem as developed by Simmons.[3,13]

The theories of Appelbaum[15,16] and Anderson[17] attribute the zero-bias anomalies to exchange scattering of the conduction electrons by localized paramagnetic states near the metal-oxide interface and are restricted to a weak-coupling regime where the anomalous tunneling current is relatively small as is the case of Ta–TaO_x–Al junctions. The anomalous conductance is given by the following expression, where J is the exchange coupling constant between the conduction electron and the magnetic impurity for electrons remaining on the same side of the junction ($J>0$, antiferromagnetic coupling):

$$\Delta G \propto -|T_J|^2 J(\rho^a)^2 \rho^b \ln\{(|eV|+kT)/E_0\}. \quad (1)$$

Here ρ^a and ρ^b are the density of states at the Fermi level in metal a and metal b, respectively, T_J is the coupling constant for a spin-flip tunnel process, and E_0 is the adjustable parameter of the theory.

For very low temperatures or for cases where the effective J is quite large, the perturbation approach used for the weak-coupling regime is invalid and nonperturbation techniques must be used. Appelbaum *et al.*[2] have made an extensive analysis of the tunneling problem using a solution to the Kondo effect given by Nagaoka.[22] They derive expressions valid for a strong-coupling regime and obtain results for the conductance due to impurity-assisted nonmagnetic tunneling, tunneling via the impurity state with spin flip, and scattering of the

[9] A. Sommerfeld and H. Bethe, in *Handbuch der Physik*, edited by H. Geiger and K. Schell (Julius Springer-Verlag, Berlin, 1933), Vol. 24/2, p. 450.
[10] R. Holm, J. Appl. Phys. **32**, 569 (1961).
[11] J. Bardeen, Phys. Rev. Letters **6**, 57 (1961).
[12] S. Shapiro, P. H. Smith, J. Nicol, J. L. Miles, and P. F. Strong, IBM J. Res. Develop. **6**, 34 (1962).
[13] J. G. Simmons, J. Appl. Phys. **34**, 1793 (1963).
[14] T. E. Hartman, J. Appl. Phys. **35**, 3283 (1964).
[15] J. Appelbaum, Phys. Rev. Letters **17**, 91 (1966).
[16] J. Appelbaum, Phys. Rev. **154**, 633 (1967).
[17] P. W. Anderson, Phys. Rev. Letters **17**, 95 (1966).
[18] A. F. G. Wyatt, Phys. Rev. Letters **13**, 401 (1964).
[19] L. Y. L. Shen and J. M. Rowell, Solid State Commun. **5**, 189 (1967).
[20] F. Mezei, Phys. Letters **25A**, 534 (1967).
[21] J. Solyom and A. Zawadowski, J. Appl. Phys. **39**, 705 (1968).
[22] Y. Nagaoka, Phys. Rev. **138**, A1112 (1965).

conduction electron back into the same side of the junction. The relative importance of these terms is governed by the relative size of the coupling parameters T_a, T_J, and J, which govern the three processes. Results derived by Appelbaum *et al.*[2] for the conductance including only terms in T_a^2 and T_J^2 are given below for $T=0$ ($T=$temperature):

$$G^{sc}=G_1^{sc}+G_2^{sc}, \tag{2}$$

where

$$G_1^{sc}(eV)=(4e^2/\pi)[T_J^2/(J\rho^a)^2]\rho^b\rho^a\{\Delta^2/[(eV)+\Delta^2]\},$$

$$G_2^{sc}(eV)=4\pi e^2T_a^2\rho^a\rho^b\{(eV)^2/[(eV)^2+\Delta^2]\};$$

Δ is given by

$$\Delta=D\exp(-1/2\,|\,J\,|\,\rho^a), \tag{3}$$

where D is the energy cutoff introduced by Nagaoka. The results given in (2) are valid for antiferromagnetic coupling ($J<0$).

For tunnel junctions in which the T_J terms are dominant a conductance peak will be observed at zero bias with an initial variation described by

$$\ln|D/(eV+k_BT)|$$

and saturating at low temperatures. For tunnel junctions in which the T_a terms are dominant a conductance minimum will be observed at zero bias and will vary initially as $\ln[(|eV|+k_BT)/D]$. As T and $V\to 0$, the conductance goes to zero. The strong-coupling theory in which the T_a terms are dominant has possible applications to our results, particularly when Al_2O_3 is present as part of the insulating barrier as, for example, the data of Figs. 2, 3, 8, 9, and 10.

For the case of very thick iron oxide barriers, however, the data suggest that some of the behavior may be consistent with standard tunnel theory and we give a brief review of the results derived by Simmons. The standard normal metal tunneling problem as developed by Simmons treats a junction with barrier height Φ and thickness s. We will discuss the development of Simmons's theory for dissimilar metals, although for the pairs of metals used in our experiments any asymmetrical effects connected with reversal of voltage polarity have been very small.

When two different metal electrodes are used with work functions ψ_2 and ψ_1, then an electric field exists within the insulating barrier given by

$$E_i=(\psi_2-\psi_1)/es, \tag{4}$$

where e is the electronic charge and s is the thickness of the insulating film. If Φ_1 is the barrier height at the interface of electrode 1 and the insulating barrier, then the barrier height Φ_2 at the interface of electrode 2 and the insulating film is given by

$$\Phi_2=\Phi_1+(\psi_2-\psi_1)=\Phi_1+\Delta\Phi. \tag{5}$$

Simmons has analyzed the case for a barrier described by formula (5) and restricted to low temperatures, where thermal excitation of current flow in the conduction band of the insulator does not contribute. Equations have been developed both for a trapezoidal barrier as shown in Fig. 13 and for a reduced barrier modified by including image forces. The shape of the modified barrier is also indicated in Fig. 13. For a trapezoidal barrier the equations obtained for the various voltage ranges are given below, where $m=$mass of electron, $e=$charge of electron, $h=$Plank's constant, $s=$thickness of insulating film, $J_1=$current density flowing from electrode 1 to electrode 2, $J_2=$current density flowing from electrode 2 to electrode 1, $V=$voltage across film, $\Phi_1=$barrier height at the interface of electrode 1 and the insulator, $\Phi_2=$barrier height at the interface of electrode 2 and the insulator, and $\Delta\Phi=\psi_2-\psi_1$.

Low Voltage: $V\approx 0$

$$J=(e^2/sh^2)[m(\Phi_1+\Phi_2)]^{1/2}V \times\exp[-(4\pi s/h)m^{1/2}(\Phi_1+\Phi_2)^{1/2}]. \tag{6}$$

This equation expresses J as a linear function of V and therefore indicates an Ohm's-law behavior at low voltages with no dependence on voltage polarity.

Intermediate Voltages: $0<V\leq\Phi/e$

For current flowing from electrode 1 to electrode 2 the current is given by

$$J_1=(e/4\pi hs^2)\{(\Phi_1+\Phi_2-eV)\times\exp[-(4\pi sm^{1/2}/h) \times(\Phi_1+\Phi_2-eV)^{1/2}]-(\Phi_1+\Phi_2+eV) \times\exp[-(4\pi sm^{1/2}/h)(\Phi_1+\Phi_2+eV)^{1/2}]\}. \tag{7}$$

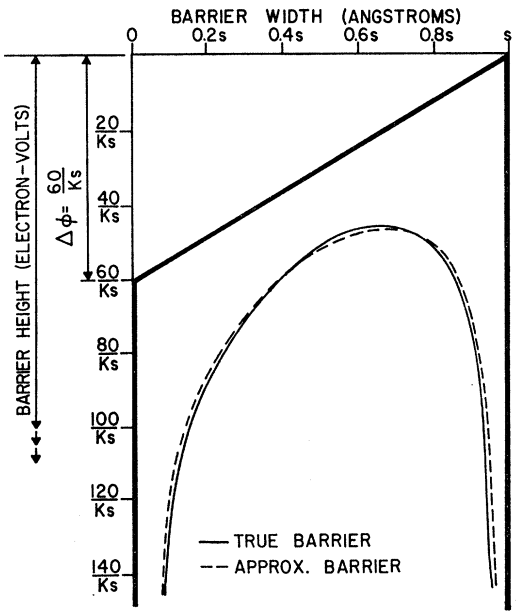

FIG. 13. Energy diagram showing the potential barrier of the oxide for dissimilar metal electrodes. The true barrier, including the effect of image charge, and the approximate barrier used by Simmons are shown, as is the trapezoidal barrier obtained when the image charge is omitted. K is the dielectric constant (see Ref. 3).

As long as $0 \leq V \leq \Phi_1/e$, $J_2 = J_1$, and the current-voltage characteristic for a trapezoidal barrier is independent of bias polarity.

High Voltages: $V > \Phi/e$

In this case there is a detectable asymmetry introduced by reversing the bias polarity and two separate equations are obtained for the forward and reverse current flow and these are given by the following expressions:

$$J_1 = \frac{1.1e(eV-\Delta\Phi)^2}{4\pi h \Phi_1 s^2} \times \left\{ \exp\left[\left(-\frac{23\pi m^{1/2}}{6h}\right)\left(\frac{s\Phi_1^{3/2}}{eV-\Delta\Phi}\right)\right] - \left(\frac{1+2eV}{\Phi_1}\right) \times \exp\left[\left(-\frac{23\pi m^{1/2}}{6h}\right)\left(\frac{s\Phi_1^{3/2}[1+(2eV/\Phi_1)]^{1/2}}{eV-\Delta\Phi}\right)\right]\right\} \quad (8)$$

and

$$J_2 = \frac{1.1e(eV+\Delta\Phi)^2}{4\pi h \Phi_2 s^2} \times \left\{ \exp\left[-\left(\frac{23\pi m^{1/2}}{6h}\right)\left(\frac{s\Phi_2^{3/2}}{eV+\Delta\Phi}\right)\right] - \left(\frac{1+2eV}{\Phi_2}\right) \times \exp\left[-\left(\frac{23\pi m^{1/2}}{6h}\right)\left(\frac{s\Phi_2^{3/2}[1+(2eV/\Phi_2)]^{1/2}}{eV+\Delta\Phi}\right)\right]\right\}. \quad (9)$$

For very high voltages such that $V \gg \Delta\Phi$, the second term in Eqs. (8) and (9) is negligible, and both equations will reduce to the Fowler-Nordheim equation for high-field tunneling given by

$$J = (BE^2/\Phi)\exp[-(\lambda\Phi^{3/2}/E)], \quad (10)$$

where

$B = 1.1e^3/4\pi h$,

$\lambda = 23\pi m^{1/2}/6he$,

$E = V/s$ = electric field in insulating layer.

When the image force is taken into account, the above formulas are modified to depend on a more complicated barrier height $\bar{\Phi}$, which includes a dependence on the dielectric constant of the insulating layer.

Simmons has made numerical evaluations of the resulting formulas and constants and Fig. 14 shows the dc tunnel resistance $R = V/J$ plotted as a function of applied voltage for an insulating barrier thickness $s = 20$ Å and dielectric constant $K = 8$. Various values of Φ_1 and $\Delta\Phi$ have been plotted. The solid curves represent the forward-bias behavior, while the dotted curves represent the reverse-bias behavior and indicate the asymmetry observed at high voltages when $\Delta\Phi \neq 0$. The solid curves labeled (a) are for $\Delta\Phi = 0$. The onset of asymmetry between the forward- and reverse-bias directions occurs for voltages $V > \Phi_1/e$. There is also a reversal in curvature of the R-versus-V curve at this point from negative to positive and for voltages on up into the Fowler-Nordheim region the curvature remains positive, $d^2R/dV^2 > 0$.

In addition to the tunnel processes treated in the above theories other mechanisms such as excitation of collective modes in the barrier could contribute to the zero-bias conductance. This problem has been considered by Duke *et al.*[23]

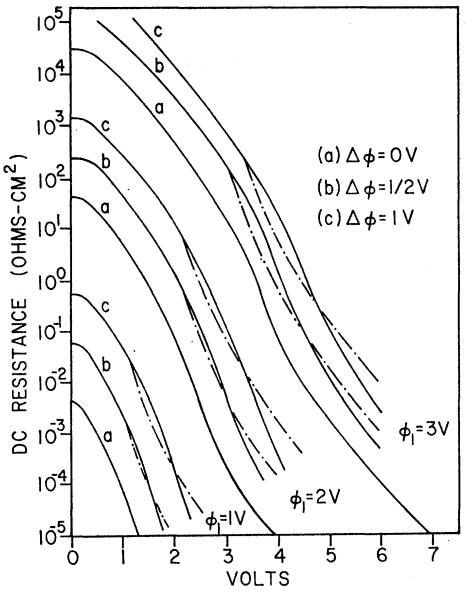

FIG. 14. dc resistance (V/J) on a logarithmic scale as a function of voltage for $s = 20$ Å and $K = 8$. These theoretical curves have been obtained from Simmons (see Ref. 3).

COMPARISON OF THEORY AND EXPERIMENT

The data obtained in these experiments have been analyzed in an effort to determine areas of agreement with the theories outlined in the previous section. At low temperatures the current-versus-voltage curves for most of the junctions show very strong deviations from Ohm's law at low voltage. Such behavior could be due either to a very low barrier height for tunneling or to anomalous processes.

In the case of Al–Al_2O_3–Al junctions Pollack and Morris[24] have carried out extensive measurements and their data indicate a barrier height of $\sim 2eV$. The present junctions using Al_2O_3 as the insulating barrier, for example, Al–Al_2O_3–Fe and Al–Al_2O_3–Fe–Al, would therefore be expected to have a rather large barrier height and consequently the strong deviations from Ohm's law at low voltage ($\ll\Phi$) could not be accounted for in terms of barrier height and are most probably due

[23] C. B. Duke, S. D. Silverstein, and A. J. Bennett, Phys. Rev. Letters **19**, 315 (1967).

[24] S. R. Pollack and C. E. Morris, Trans. Met. Soc. AIME **233**, 497 (1965).

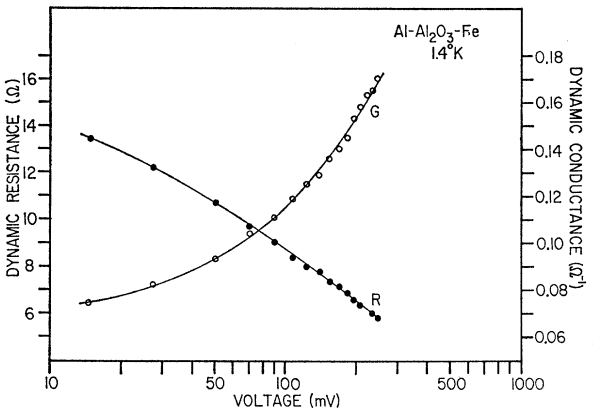

(a)

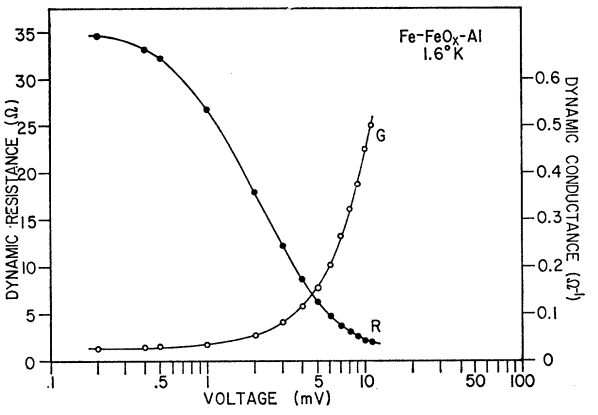

(b)

FIG. 15. Dynamic resistance and dynamic conductance versus the logarithm of the voltage for an Al–Al_2O_3–Fe junction at 1.4°K and an Fe–FeO_x–Al junction at 1.6°K.

to anomalous tunneling mechanisms. On the other hand, for junctions with only FeO_x as the barrier a relatively low barrier height is a possibility and this could be a major factor, although anomalous conductance may also be contributing.

The anomalous tunneling theories generally predict an initial dependence of the tunnel conductance on the logarithm of the voltage and temperature. We have plotted both the conductance and the dynamic resistance of our junctions versus the logarithm of the voltage and semilog plots for typical junctions are shown in Fig. 15. All of the plots show deviations from purely logarithmic behavior and this is also true of the temperature dependence. (See, for example, Fig. 4.) We can, however, obtain a better empirical fit to the data by fitting to higher powers of the logarithm. The logarithmic dependence predicted by the theory applied only to the anomalous part of the conductance and other contributions could account for the deviations from logarithmic behavior observed for the total conductance. However, at present we are unable to obtain a sufficiently quantitative agreement in order to establish an anomalous behavior as described by the theory of Appelbaum *et al.*[2]

For the pure FeO_x barriers we have also approached the problem using standard tunnel theory as developed by Simmons[3,13] in order to see how much of the data can be fitted by allowing a low barrier height to account for the strong deviations from Ohm's law. Various thermal processes could then account for the strong temperature dependence. Comparison with Simmons's development will be discussed below.

In Fig. 16 we show a semilog plot of the dc resistance versus applied voltage for seven different Fe–FeO_x–(Fe, Al, Ag) junctions representing a range of increasing resistance values obtained by increasing the time and temperature of oxidation used in preparation. For the high-resistance junctions the curvature (d^2R/dV^2) over the entire accessible range of voltage is positive. Assuming that Simmons's theory completely describes these junctions, comparison to the theoretical curves of Fig. 14 indicates that the applied voltage is greater than Φ_2/e even at the lowest measured voltages. For most of the high-resistance junctions our present apparatus does not allow us to accurately measure the characteristic at sufficiently low voltage to observe a reverse in curvature and an approach to Ohm's-law behavior. A number of the low-resistance junctions only show a reverse of curvature and an approach to Ohm's-law behavior at very low voltages and these are also shown in Fig. 16. The resistance-versus-voltage curves for these low-resistance junctions have a change in curvature at unusually low voltages, indicating that simple barrier analysis may not be valid for them. The junctions described above and shown in Fig. 16 will be denoted as type I.

A few of the low-resistance junctions as well as several of the high-resistance junctions do, however, show a distinct reversal of curvature and an Ohm's-law behavior over a larger range of voltage and examples are shown in Fig. 17. These will be denoted as type II and a junction showing this type of dc resistance versus voltage characteristic also shows a much smaller temperature dependence of resistance than that observed for the type-I junctions.

The observations on type-I junctions indicate that in order to describe the behavior by standard tunnel processes the barrier height Φ_2/e must be assumed to be very small—considerably less than 0.1 eV since no reversal of curvature in the resistance-versus-voltage plot is observed down to very low voltages in the case of high-resistance junctions. An exact estimate is difficult since we do not at present have a detailed and reliable measurement of oxide thickness. However, several other observations also indicate a very low value for the barrier height.

For example, measurements of the tunnel current flow in the high-voltage Fowler-Nordheim region also provide an estimate of barrier height. We have plotted

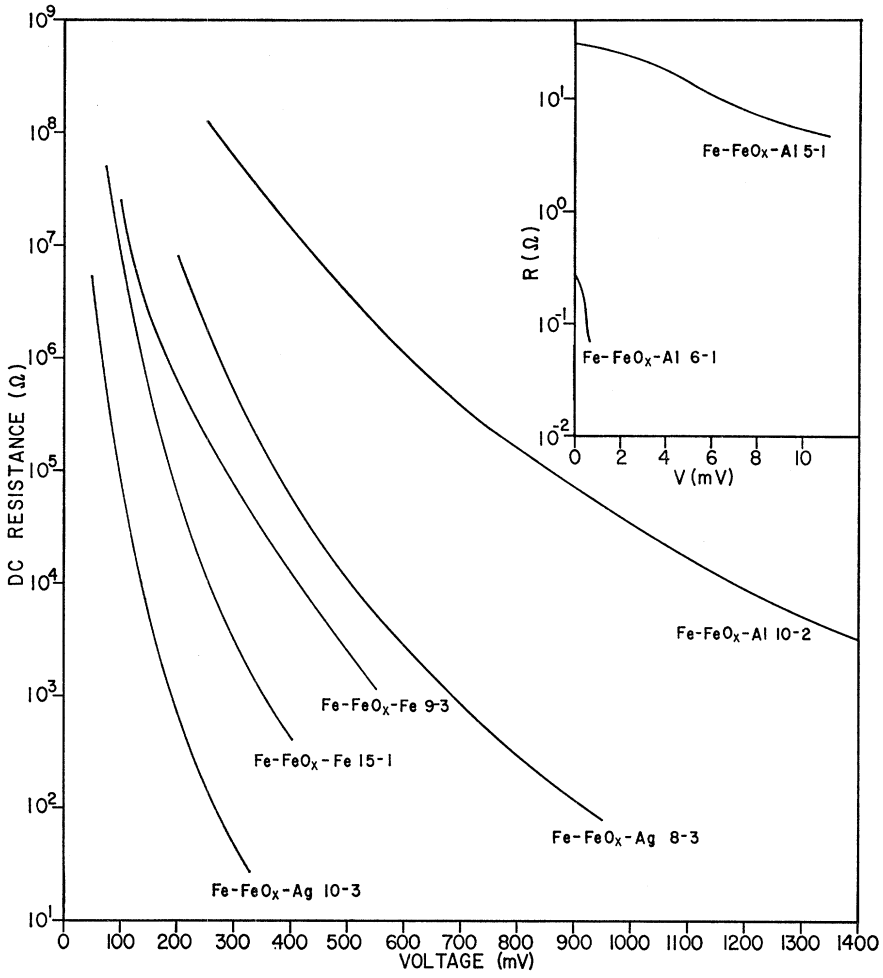

FIG. 16. dc resistance (V/I) on a logarithmic scale as a function of voltage at 4.2°K for seven type-I junctions.

the data for the junctions of Fig. 16 on an I/V^2-versus-$1/V$ plot and the results are shown in Fig. 18. The Fowler-Nordheim region would correspond to a straight line on such a plot. The data indicate an approach to a straight-line behavior, and a reasonably accurate slope can be estimated at high voltages. The high-voltage ranges for the curves of Fig. 18 are limited, however, by the onset of breakdown, which usually occurs for applied voltages above some critical value. As a consequence we probably do not reach the region where the second term in Eqs. (8) or (9) is completely negligible.

We have estimated the slopes for the high-voltage region of the curves shown in Fig. 18, and the values are listed in Table I. For a constant barrier height the slopes would be proportional to the thickness of the oxide layer and the order of values in Table I is in agreement with this, although no direct thickness measurement has been made. We have, however, used the oxidation data for iron cited by Tomashov and shown in Fig. 1 to obtain an estimate of the various oxide layer thicknesses and these values are listed in Table I. Assuming the free-electron effective mass, we have calculated the barrier height using the Fowler-Nordheim slope and these values are also listed in Table I. All of the junctions show reasonable consistency and the calculated barrier heights range from 0.012–0.038 eV with an average value of 0.025 eV. In applications of the Fowler-Nordheim equation to simple junctions[25]

TABLE I. Values of the slope m and calculated barrier height ϕ derived from the Fowler-Nordheim plots shown in Fig. 18 for various junctions with FeO_x insulating barriers.

Sample		s (Å)	m (V)	Φ (mV)
Fe–FeO_x–Ag	8-3	1500	−6.5	34
Fe–FeO_x–Fe	9-3	4000	−3.8	12
Fe–FeO_x–Al	10-2	2000	−10	38
Fe–FeO_x–Ag	10-3	1000	−1.8	19
Fe–FeO_x–Fe	15-1	1500	−3.1	21

[25] T. E. Hartman and J. S. Chivian, Phys. Rev. **134**, A1094 (1964).

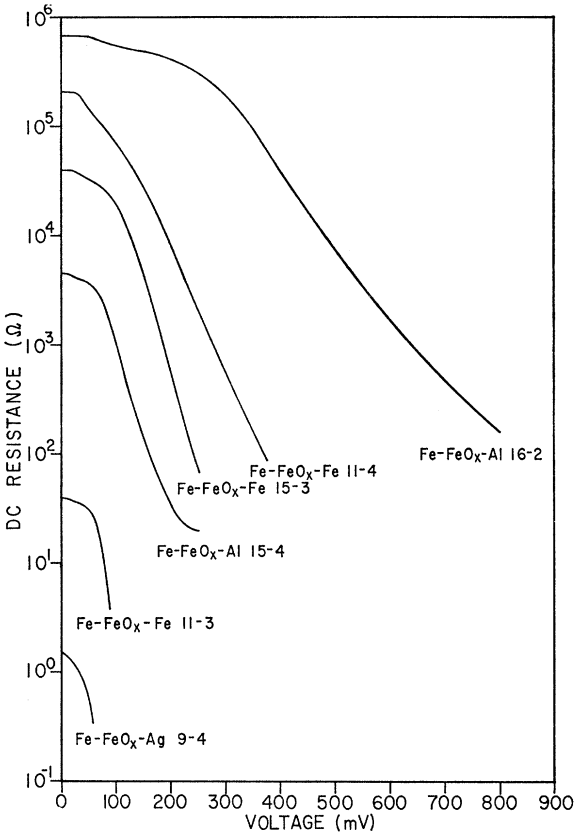

FIG. 17. dc resistance (V/I) on a logarithmic scale as a function of voltage at 4.2°K for six type-II junctions.

for voltages ten times the barrier height the Fowler-Nordheim plot show excellent linear behavior. The junctions reported here only approach linear behavior at these voltages, indicating that the characteristics are not those of a simple junction but rather those of an unusual barrier and/or zero-bias anomalies.

If a low value of the barrier height is assumed to be a controlling factor, then one would perhaps expect to see strong thermal effects by the time the temperature reaches 77°K, where $kT \approx 0.006$ eV. This would certainly reduce the effective tunnel barrier and modify the tunnel resistance substantially. However, the enormous drop in zero-bias resistance between 4.2 and 77°K may also be connected with the ordering transition in magnetic iron oxide Fe_3O_4. Fe_3O_4 is generally considered to have a spinel-type structure containing two crystallographic positions in which the metal ions are octahedrally coordinated by the oxygen ions.[26,27] One of these positions contains ions both in the divalent and trivalent state. For the stoichiometric composition at low temperatures these ions are distributed according to an ordered state, while at high temperatures this long-range order is substituted by a short-range order showing an anomalously high conductivity (a resistivity of 10^{-2} Ω cm at room temperature). The much higher conductivity at higher temperatures is due to the decrease in activation energy for transfer of an electron from an Fe^{2+} to a neighboring Fe^{3+} in the disordered state.

This transition from long-range to short-range order could well explain the rapid decrease in zero-bias resistance of our junctions at higher temperatures. For stoichiometric Fe_3O_4 the transition temperature has been measured by Verwey and Haayman[27] to be 120°K with an estimated activation energy for electron transfer in the disordered state of less than 0.1 eV. Verwey and Haayman also find that excess oxygen lowers the transition temperature and causes the transition to be less sharp. Most of our data indicate that a rapid rise in conductivity has set in by 77°K, possibly indicating that excess oxygen is present. In addition to Fe_3O_4, other compositions of FeO_x are

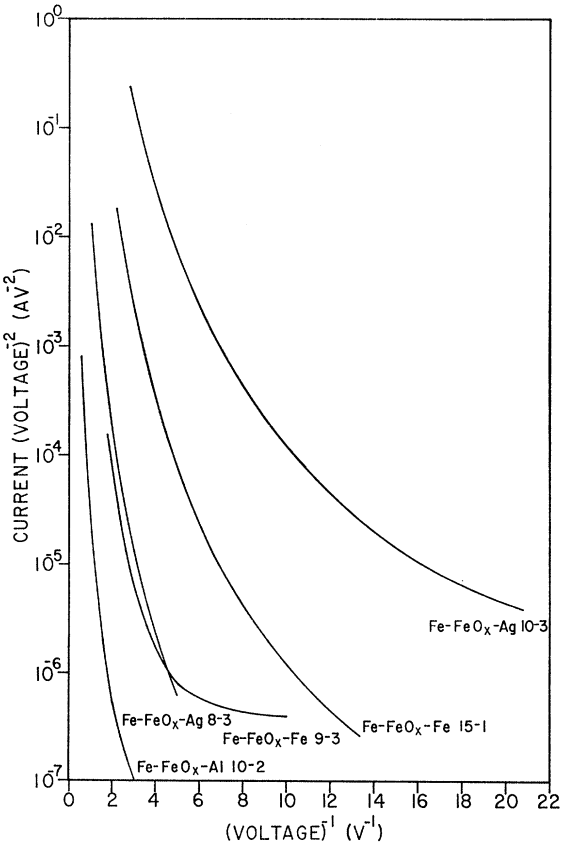

FIG. 18. Fowler-Nordheim plot, $\log I/V^2$ versus $1/V$, for five type-I junctions.

[26] E. J. W. Verwey, in *Semiconducting Materials*, edited by H. K. Henisch (Butterworths Scientific Publications Ltd., London, 1951), p. 151.
[27] E. J. W. Verwey and P. W. Haayman, Physica 8, 979 (1941).

probably present in the films and this might modify the pure magnetic oxide (Fe_3O_4) behavior. For a check we oxidized one of our films completely to iron oxide and measured the resistivity at room temperature. A value of 10^{-2} Ω cm was obtained, in agreement with the expected value for magnetic iron oxide Fe_3O_4.

Since the iron oxide layers are probably a mixture of several phases of iron oxide, this may also play some role in producing the two distinct types of behavior that we observe. For example, Fe_2O_3 is a relatively good insulator with a resistivity of the order of 10^{11} Ω cm at room temperature and probably has a substantially larger barrier height for tunneling than that of Fe_3O_4 (magnetic iron oxide). If the oxidation of the iron proceeds in such a way that a reasonably continuous film of Fe_2O_3 is formed, then the larger barrier height would be expected to contribute and it would be possible to observe an approach to Ohm's-law behavior at low voltages (type II). If, on the other hand, most of the effective tunnel barrier is Fe_3O_4, the low barrier will dominate and the type-I behavior will be observed.

The oxidation of iron proceeds in a rather nonuniform fashion and exact control of the effective tunnel barrier is therefore difficult since it requires close control of the oxidation process. We hope to develop some techniques for doing this, but the present experiments have not been controlled sufficiently to check the above hypothesis in detail.

CONCLUSIONS

In this paper we have reported results of measurements on tunnel current flow in junctions using ferromagnetic metal oxides as the insulating barrier. We have also made measurements on junctions with Al_2O_3 barriers containing iron impurities deposited at the Al_2O_3–Al interface. All of these junctions have shown large deviations from Ohmic behavior at very low voltages and the tunnel conductance has shown a strong temperature dependence extending down to temperatures as low as 1°K. These features have been investigated in particular detail for junctions made from iron and iron oxide with the second electrode made from aluminum, silver, and iron. A number of general statements can be made regarding the behavior of the iron or iron-doped junctions and these are listed below.

(1) The non-Ohmic behavior for these junctions is so strong that the characteristic curves are similar to those predicted for anomalous tunneling due to magnetic impurities in the junction.

(2) The temperature and voltage dependence of the tunnel conductance, however, do not agree in sufficient quantitative detail with the logarithmic dependence predicted by the theories of anomalous tunneling to conclude that definite scattering from magnetic impurities is occurring.

(3) The Al–Al_2O_3–Al junctions, when doped with iron, do, however, show a large zero-bias anomaly, which is simply added to the characteristic of the identical undoped junction. This system would therefore appear to be the simplest one studied in the present group of experiments and can be generally understood in terms of an anomalous scattering mechanism near zero bias.

(4) The junctions using FeO_x barriers appear more complicated, although they also show a strong zero-bias anomaly corresponding to a resistance maximum.

(5) The results on junctions using iron oxide barriers have also been compared to standard tunneling theory. Assuming that a standard tunneling process is dominant, a qualitative fit of the data can be obtained with a very low barrier height. The qualitative fit obtained would not be particularly meaningful, however, if a substantial anomalous component were present in the tunneling current. In any case the low barrier height seems to be required in order to explain the data on very thick FeO_x barrier junctions (>1000 Å).

(6) An estimate of the barrier height has been obtained by fitting the FeO_x data to a Fowler-Nordheim high-field tunneling equation. For the seven junctions analyzed, the average barrier height calculated is 0.025 eV.

(7) At helium temperatures the junctions with iron oxide barriers show an interesting "breakback" effect above some critical voltage. This corresponds to a sudden decrease in the voltage required to maintain a given current above the critical value.

(8) The "breakback" behavior shows a hysteresis effect that increases as the temperature is lowered below 4.2°K.

(9) The "breakback" behavior is reproducible over many cycles provided the current does not become too high and such behavior may have applications to low-temperature devices.

(10) The junctions with iron oxide barriers show an extremely rapid temperature dependence between helium and nitrogen temperature, and even below 4.2°K the temperature dependence is easily observable. This is consistent with a very low barrier height, but some aspects of the behavior may also be associated with an order-disorder transition in magnetic iron oxide Fe_3O_4.

(11) A number of the iron oxide junctions show an observable Ohmic behavior and we suggest that this may be associated with barriers formed from other phases of iron oxide besides Fe_3O_4.

In addition to the results on iron, preliminary data on junctions using cobalt and nickel have also been reported and these show some characteristics similar to those reported for iron. The voltage and temperature dependence are much less dramatic, however.

Finally, we would like to say that the conclusions listed above are meant to summarize our results and should not be considered as final. The behavior of these junctions appears sufficiently interesting, however, that further work should be done in order to understand the behavior more fully.

ACKNOWLEDGMENTS

The authors would like to acknowledge many interesting and stimulating discussions with Dr. J. Appelbaum, Dr. J. Rowell, Dr. L. Shen, Dr. C. Duke, and Dr. A. Bennett. We would also like to thank Professor L. Falicov, Professor Zuckermann, Professor V. Celli, Professor N. Cabrera, and Professor R. Ferrell for continuing and stimulating interest in the research. We would also like to acknowledge the contribution of P. Sommer and W. Frewer to the construction of the equipment.

PHYSICAL REVIEW VOLUME 172, NUMBER 2 10 AUGUST 1968

Symmetry of the Wave Functions in the Band Theory of Ferromagnetic Metals*

L. M. FALICOV† AND J. RUVALDS

Department of Physics and James Franck Institute, University of Chicago, Chicago, Illinois 60637

(Received 12 January 1968)

The symmetry of wave functions in the one-electron band theory of ferromagnetic solids is discussed. The exchange interaction, spin-orbit coupling, and coupling of spins to the magnetic induction vector **B** are included in the Hamiltonian. The resulting symmetry, which is not invariant under time reversal, can contain only those point operations which belong to the paramagnetic space group and leave the pseudovector **B** invariant at the same time. Character tables are presented for the case of face-centered cubic, body-centered cubic, and hexagonal close-packed structures and for various directions of **B**. Compatibility relations and lifting of degeneracies are discussed.

I. INTRODUCTION AND GENERAL THEORY

IN the last few years the band theory of solids has been considerably successful in explaining the properties of the ferromagnetic metals.[1] In particular the group-VIII transition metals Fe, Co, and Ni have been the subject of many investigations, both theoretical[2–12] as well as experimental,[13–19] which exhibit in a prominent way the band-theoretical aspects of the behavior of their conduction electrons.

It is important to remark, however, that in the ferromagnetic metals, which crystallize in the usual metallic structures fcc (Ni), bcc (Fe), and hcp (Co), the usual group-theoretical arguments,[20–22] which refer to nonmagnetic materials, are no longer valid. For instance, the presence of a net magnetization results in the destruction of time-reversal symmetry[23] with the consequent splitting of up and down spin bands. The effects of the broken symmetries, moreover, go beyond this first-order and most important feature; in addition to time reversal, many other symmetry operations cease to exist in the presence of ferromagnetism. It is the purpose of this paper to reexamine the question of band symmetries in those circumstances and to provide the necessary character tables and compatibility relations which give complete information on the symmetry properties of the electronic states in ferromagnetic metals.

In the one-electron approximation, the electrons in a

* Work supported in part by the National Science Foundation and the National Aeronautics and Space Administration.

† Alfred P. Sloan Research Fellow.

[1] For a complete reference to the many contributions to the itinerant electron theory of magnetism, see C. Herring, in *Magnetism*, edited by G. T. Rado and H. Suhl (Academic Press Inc., New York, 1966), Vol. 4.

[2] J. H. Wood, Phys. Rev. **126**, 517 (1962).

[3] S. Wakoh and J. Yamashita, J. Phys. Soc. Japan **21**, 1712 (1966).

[4] L. F. Mattheiss, Phys. Rev. **134**, A970 (1964).

[5] J. Yamashita, M. Fukuchi, and S. Wakoh, J. Phys. Soc. Japan **18**, 999 (1963).

[6] J. G. Hanus, MIT Progress Report No. 44, 1962, p. 29 (unpublished).

[7] E. C. Snow, J. T. Waber, and A. C. Switendick, J. Appl. Phys. **37**, 1342 (1966).

[8] L. Hodges, H. Ehrenreich, and N. D. Lang, Phys. Rev. **152**, 505 (1966).

[9] J. C. Phillips, Phys. Rev. **133**, A1020 (1964).

[10] S. Wakoh, J. Phys. Soc. Japan **20**, 1894 (1965).

[11] H. Ehrenreich, H. R. Philipp, and D. J. Olechna, Phys. Rev. **131**, 2469 (1963).

[12] J. W. Connolly, Phys. Rev. **159**, 415 (1967).

[13] J. R. Anderson and A. V. Gold, Phys. Rev. Letters **10**, 277 (1963).

[14] E. Fawcett and W. A. Reed, Phys. Rev. **131**, 2463 (1963).

[15] A. S. Joseph and A. C. Thorsen, Phys. Rev. Letters **11**, 554 (1963).

[16] D. C. Tsui and R. W. Stark, Phys. Rev. Letters **17**, 871 (1966).

[17] D. C. Tsui, Phys. Rev. **164**, 669 (1967).

[18] W. A. Reed and E. Fawcett, J. Appl. Phys. **35**, 754 (1964).

[19] L. Hodges, D. R. Stone, and A. V. Gold, Phys. Rev. Letters **9**, 655 (1967).

[20] L. P. Bouckaert, R. Smoluchowski, and E. P. Wigner, Phys. Rev. **50**, 58 (1936).

[21] C. Herring, J. Franklin Inst. **233**, 525 (1942).

[22] R. J. Elliott, Phys. Rev. **96**, 280 (1954).

[23] C. Herring, Phys. Rev. **52**, 361 (1937).